

P-type $\text{Cu}_2\text{ZnSnS}_4$ as Multifunctional Material for Photovoltaic and Thermoelectric Application: Theoretical Investigation

($\text{Cu}_2\text{ZnSnS}_4$ Jenis-*p* sebagai Bahan Pelbagai Fungsi untuk Aplikasi Photovolta dan Termoelektrik: Siasatan Teori)

Hassan Ahmoum^{a,*}, Mourad Boughrara^a, Mohamed Kerouad^a
^a Faculty of Sciences, University Moulay Ismail, Morocco

Puvaneswaran Chelvanathan^b, Kamaruzzaman Sopian^b, Mohd Sukor Su'ait^{b*}
^b Solar Energy Research Institute (SERI), Universiti Kebangsaan Malaysia, Malaysia

Lee Tian Khoon^{c*}
^c Fuel Cell Institute, Universiti Kebangsaan Malaysia, Bangi, Malaysia

Baohai Jia^d, Guojian Li^d
^d Key Laboratory of Electromagnetic Processing of Materials (Ministry of Education), Northeastern University, China

ABSTRACT

In this work, a detailed information about physical properties of $\text{Cu}_2\text{ZnSnS}_4$ stannite phase by first principles calculation has been presented. Using density functional theory based on the generalized gradient approximation GGA, the structural properties such as lattice parameters and bulk modulus has been determined. In addition, structure electronic and partial density of state to characterize the electronic properties was also calculated. For the optical properties investigation, the absorption coefficient and the efficiency of energy conversion has been calculated. Finally, we have investigated on thermoelectric properties such as electrical conductivity, Seebeck coefficient, thermal conductivity and figure of merit to evaluate the potential of this material in different applications. From our results presented herein, we conclude that this material can be considered potential multifunctional material for thermoelectric and photovoltaic applications.

Keywords: $\text{Cu}_2\text{ZnSnS}_4$ first principles study; material modeling, photovoltaic; thermoelectric

ABSTRAK

Dalam kajian ini, sifat fizikal $\text{Cu}_2\text{ZnSnS}_4$ berfasa stanit telah dijalankan dengan menggunakan pengiraan prinsip pertama telah dipersembahkan dengan terperinci. Dengan menggunakan teori fungsi kepadatan (DFT) yang berdasarkan kepada anggaran kecerunan umum (GGA), sifat struktur seperti tenaga kekisi dan modulus pukal $\text{Cu}_2\text{ZnSnS}_4$ telah ditentukan. Selain itu, sifat elektronik $\text{Cu}_2\text{ZnSnS}_4$ ini ditentukan melalui pengiraan terhadap struktur elektronik dan ketumpatan keadaan separa (partial density of state). Sifat optik $\text{Cu}_2\text{ZnSnS}_4$ juga telah disiasat melalui pengiraan terhadap pekali serapan dan kecekapan penukaran tenaga. Akhir sekali, kami juga menyiasat pekali Seebeck, kekonduksian terma dan angka merit untuk mencungkil potensi bahan ini dalam aplikasi lain. Daripada hasil kajian yang telah diperolehi, kami boleh menyimpulkan bahawa bahan ini mempunyai potensi dan peranan sebagai bahan kepelbagaian fungsi dalam aplikasi terma elektrik dan fotovoltai.

Kata kunci: $\text{Cu}_2\text{ZnSnS}_4$; kajian prinsip pertama; pemodalan bahan, fotovoltai; terma elektrik

INTRODUCTION

Solar energy has been considered one of the most feasible solution to compensate the energy consumed on the whole planet by harvesting the sunlight and converting the solar energy to electricity by using the photovoltaic technology. Moreover, hybridization of photovoltaic (PV) and thermoelectric (TE) technology device has long been considered ideal for efficient harnessing solar energy. The TE is technology which allow its material to transfer a gradient thermal energy and converting it to electrical energy

(Mohamed et al. 2016). The combination of PV-TE technology is very important as it can utilize the full spectrum of solar energy via lossless coupling between PV and TE device through the collection of waste energy from thermalization and transmission losses from PV device, which subsequently, provides the maximum (or near maximum) power output (Park et al. 2013).

In terms of material used, chalcogenide alloys such as $\text{Cu}(\text{In,Ga})\text{Se}_2$ (CIGS), $\text{Cu}_2\text{ZnSnS}_4$ (CZTS) and GaAs are interesting to be studied (Sakib & Ahad 2018). $\text{Cu}(\text{In,Ga})\text{Se}_2$ (CIGS) is already integrated in the commercial solar cell

because of its high conversion energy which has already achieved efficiency of 20.8% (Jackson et al. 2014). While $\text{Na}_{0.2}\text{Pb}_{0.8}\text{Te}$ is the most used material in the thermoelectric device and it has higher figure of merit around 1.74 at 774 K (Wang et al. 2013). However, the high cost and toxicity of these elements are the main concerns and responsible for the high price of these conversion materials. In order to meet the challenges of low cost PV and TE devices, the need to explore other materials and alternatives are inevitable. For this reason, we have investigated on the $\text{Cu}_2\text{ZnSnS}_4$ (CZTS) because of various advantages such as earth abundant and environmentally friendly component elements (nontoxic elements Cu, Zn, S and Sn), optimal direct band gap (1.5 eV), high absorption coefficients 10^5 cm^{-1} (Ricardo et al. 2013) and it is a semiconductor with *p*-type conductivity (Olgar et al. 2017). Consequently, CZTS has already found in several technologies such as photovoltaic (Mahajan et al. 2018), thermoelectric (Kumar et al. 2018) and photocatalysis (Hou et al. 2014). In fact, CZTS is considered one of the most explored material in the recent years, by experimental and computational methods. For example, Reshak et al. (2014) have investigated on the electronic and optical properties of kesterite CZTS by mean of density functional theory (DFT) and they have showed that this material can be used as an absorption material because of the value of band gap. On the other hand, Liu et al. (2009) have investigated on the thermoelectric properties of kesterite phase of $\text{Cu}_2\text{ZnSnQ}_4$ ($Q = \text{S}, \text{Se}$) and they have showed that CZTS can be used as a *p*-type thermoelectric material. As we know, CZTS material generally exists in two types of crystal structures, *i.e.*, kesterite and stannite with space group of *I*-4 and *I*-4 2m, respectively (Quennet et al. 2017). Most of the DFT studies have been focused on the kesterite structure. However, many researchers, by experimental, have synthesis the CZTS with the presence of two phases (stannite and kesterite). While, other researchers have synthesis CZTS with pure stannite phase. The knowledge of the physical properties of stannite phase by DFT is obligatory, especially to the best of our knowledge, there are no papers published on thermoelectric study related to stannite CZTS. For this reason, in this paper, we explored the crystalline structure, electronic, electrical, optical and thermoelectric properties of stannite CZTS. By using the first principal approach, we calculated the properties of stannite CZTS. The relationship between photovoltaic and thermoelectric performance will be discussed in this paper, and a possible explanation for previous experimental observations will be provided. This work should and will help to deepen understand on stannite CZTS compound.

METHODOLOGY

In this study, we performed a computational method where a supercell of CZTS stannite compound with space group symmetry of *I*-4 2m (no. 121) as shown in Figure 1 were considered. All calculations were carried out by using the first-principles pseudopotential method based on the DFT and the plane-wave method implemented in Quantum-

espresso package (Giannozzi et al. 2009). Exchange and correlation effects are treated under the generalized-gradient-approximation with Perdew-Burke-Ehrenkof (PBE) functional (Perdew et al. 1996) and the ultrasoft pseudopotential (USP) method was used to treat the valence electron configuration ($3d_{10}4s_1$ for Cu, $3d_{10}4s_2$ for Zn, $4d_{10}5s_25p_2$ for Sn, $3s_23p_4$ for S). The cut-off for the kinetic energy was set at 40 Ry and the charge density cut-off was set at 320 Ry. A $4 \times 4 \times 4$ Monkhorst-Pack grid was used to set the *k*-point sampling (Monkhorst et al. 1976), the convergence threshold for self-consistent-field iteration was set at 10^{-7} eV.

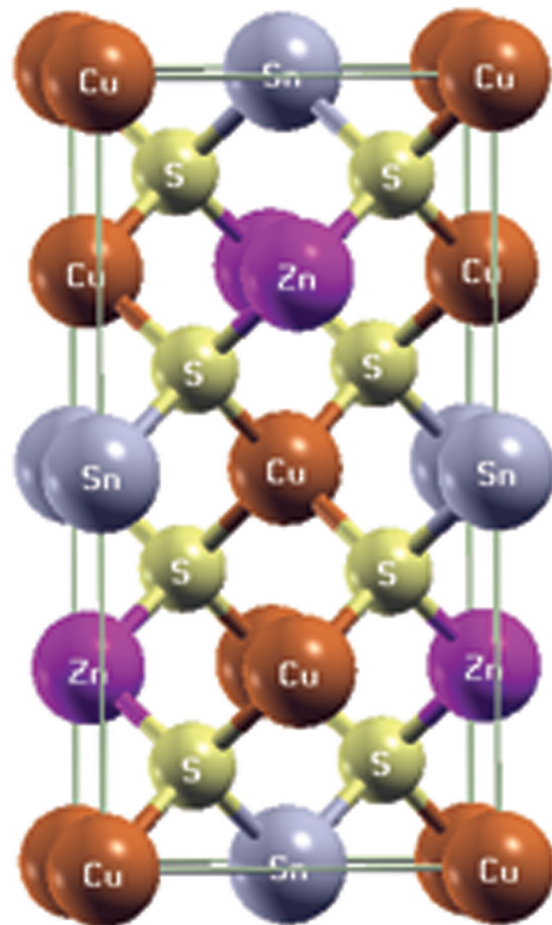


FIGURE 1. The optimized crystalline structure of CZTS stannite phase

RESULTS AND DISCUSSION

STRUCTURAL PROPERTIES

The most important part in the DFT calculation is to obtain the optimized lattice parameters because all the physical properties are relied to the crystal structure. In order to obtain the optimized structural properties in the ground state, such as the equilibrium lattices constant (a_0), (c_0), bulk modulus (B_0) and bulk modulus pressure derivative B' of stannite CZTS compound, we have calculated the total energy for different volume of the material, then we have fitted our data with the Murnghan method as shown in Figure 2.

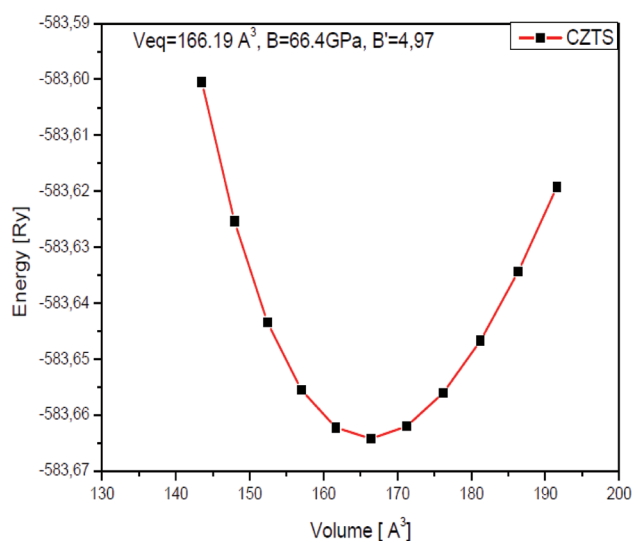


FIGURE 2. Energy versus volume

According to the results, the lattice parameters of pure CZTS are $a_0 = 5.50$ $c_0 = 10.98$ Å, and this result are close to the theoretical value found by Zhao et al. (2017) which are $a_0 = 5.48$ $c_0 = 10.96$ Å. Whereas, the experimental results show that CZTS possessed of $a_0 = 5.449$ $c_0 = 10.757$ Å lattice parameters (Gusain et al. 2014). The differences between the DFT results with the experimental results are that the method generalized gradient approximation (GGA) that we have used for calculation is always considering of overestimated the value of the equilibrium lattice parameter. Finally, our value of the bulk modulus is in excellent agreement with the values obtained by Zhao et al. (2017) which is 64.39 GPa. From these results, we conclude that our method of calculations is feasible and reliable.

ELECTRONIC PROPERTIES

The electronic structure is an important parameter to understand the physical properties of this material. In light of this, we conducted investigation on the electronic properties of the $\text{Cu}_2\text{SnZnS}_4$ and the results are depicted in Figure 3.

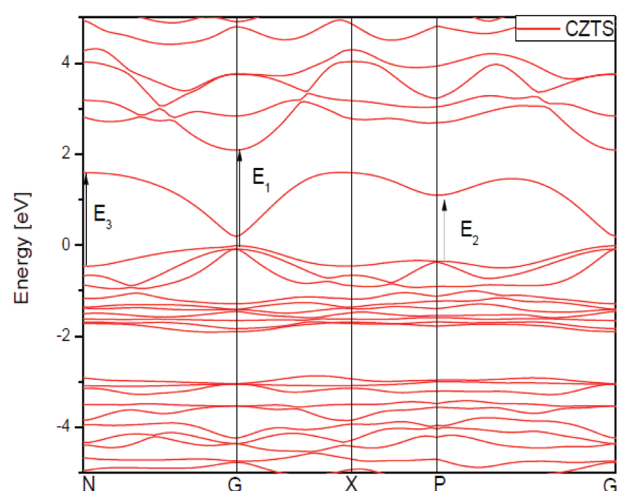


FIGURE 3. Electronic Structure of stannite CZTS

The fermi level for pure CZTS is on the top of the valence band, which means that this material is a non-degenerate semiconductor, and exhibits a direct band gap, because the conduction band minimum and the valence band maximum are both located at G point (center of the first Brillouin zone). The calculated band gap of pure CZTS is 0.204 eV, which is close to results found by Mounkachi et al. (2014) (0.2 eV). However, this value was found to be much less than the experimental value (1.5 eV) and that's due to the fact of limitation of DFT in GGA. The discontinuity in the exchange correlation potential is not considered within the framework of DFT (Anisimov et al. 1997). To go in depth, we have calculated the partial density of states and total one TDOS of pure CZTS as shown in Figure 4, where we can observe that the conduction band is formed by the hybridization of $4s$ -Cu, $5s$ -Sn, $5p$ -Sn and $4s$ -Zn states, and the valence band is formed by the hybridization between $3p$ -S and $3d$ -Cu states. As we know, the physical properties of materials are determined only with the bottom of conduction band and with the maximum valence band. For this reason and to be more specification in this compound the bottom of conduction band is formed essentially by $5s$ -Sn states, and the maximum valence band is formed by $3d$ -Cu states.

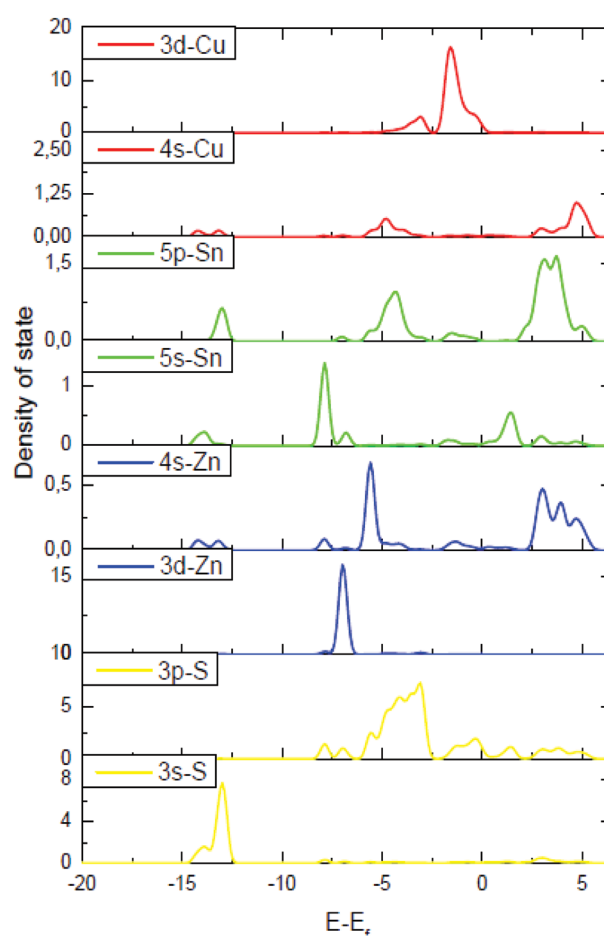


FIGURE 4. Partial density of states

It's well known that good absorption material for photovoltaic application should have a high value of coefficient absorption in the visible region. To reach this aim, we have calculated firstly the imaginary and real part of complex dielectric function $\epsilon(\omega) = \epsilon_r(\omega) + i\epsilon_i(\omega)$ with $\epsilon_r(\omega)$ with represents the real part of dielectric function which characterizes the transition intra-band, and $\epsilon_i(\omega)$ represents the imaginary part of dielectric function which characterizes the transition inter-band. We have calculated the absorption coefficient $\alpha(\omega)$ of the stannite CZTS by using Equation (1):

$$\alpha(\omega) = \sqrt{2\omega} \sqrt{\sqrt{\epsilon_r^2(\omega) + \epsilon_i^2(\omega)} - \epsilon_r(\omega)} \quad (1)$$

It is known that the DFT usually does not understand the energy gaps with respect to the experimentally obtained gaps as we have seen in electronic structure. To get the appropriate results for optical properties, we have corrected the optical band gap by adding a scissor shift and its value is 1.26 eV. The scissor shift is the difference between the calculated and measured energy gaps. In Figure 5 we have presented the absorption coefficient in the wavelength range between 300 and 1200 nm. We can see clearly (in Figure 5) the presence of 3 regions. The first region is with high absorption coefficient under 550 nm, the value of α is in order of 10^5 cm^{-1} , in which this value confers the characteristic of CZTS of high absorption. The second region is between 550 nm and 800 nm which the value of α is in the order of 10^4 cm^{-1} . This value is also considered a good adsorption property for the photovoltaic application. These two regions are corresponding to fundamental absorption due to the inter-band of electronic transition. Finally, we have a third region above of 800 nm in which the absorption coefficient become null. In this region, the energy of photon incident is lower than the energy of band gap which doesn't cause any electronic transition between localized states.

Moreover, we noticed the existence of two peaks, the first one is at 388 nm which corresponds to the 3.27 eV and by removing the scissor added, we have found after analyzing the structure electronic that the transitions correspond to this peak are $E1$ and $E3$. We can remark that, $E1$ is the transition between the carrier's charges from the maximum valence band to the second conduction band. From PDOS (Figure 4), we found that this transition corresponds to transition of carrier's charges from $3d\text{-Cu}$ and $3p\text{-S}$ states to $5p\text{-Sn}$ and $4s\text{-Zn}$ states. $E3$ is the transition in the high point symmetry N which is originated from the electron transition between $3d\text{-Cu}$ and $3p\text{-S}$ to $5s\text{-Sn}$ and $3p\text{-S}$ states. In addition, these transitions are all naturally direct, which is profitable to the photovoltaic application. With the same logical, the second peak appears at 474 nm is correspond to the transition $E2$, which is originated from $3d\text{-Cu}$ and $3p\text{-S}$ states to $5s\text{-Sn}$ and $3p\text{-S}$ states. The variation of the absorption coefficient α versus the energy of excitation is used to determine the optical band gap, by using the Tauc's relation in Equation (2):

$$\alpha hv = A(hv - E_g)^{1/2} \quad (2)$$

where A is a constant for direct transition and (hv) is the energy of the incident photon. In Figure 6, we have presented the variation of $(\alpha hv)^2$ versus photon energy (hv) . The calculated optical band gap with our method is 1.46 eV, which is in excellent accord with experimental value (Olgar et al. 2017).

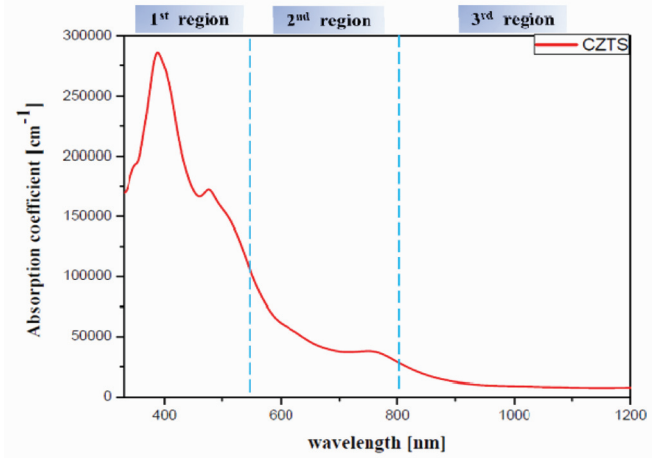


FIGURE 5. Absorption coefficient of simulated CZTS

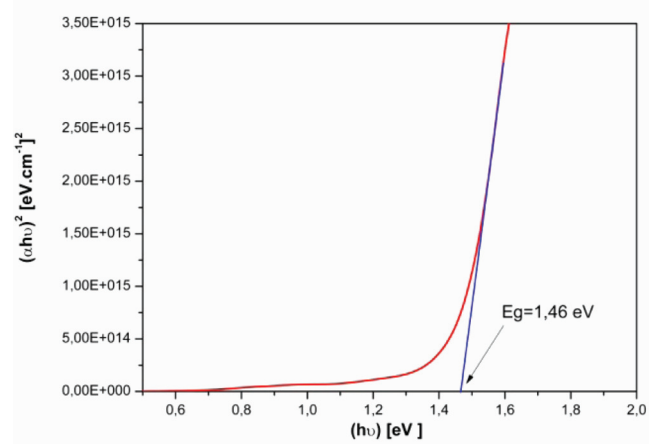


FIGURE 6. Optical band gap of simulated CZTS

PHOTOVOLTAIC PERFORMANCE

To complete our study on photovoltaic performance we have calculated the characteristic J - V to extract the short circuit current density J_{sc} , the reverse saturation current density J_0 , power density P , open circuit voltage V_{oc} and finally the efficiency conversion energy h of the absorber materials under the excitation of the standard AM1.5G solar spectrum at 300 Kelvins. P_m can be obtained from the J - V characteristic of the solar cell in Equation (3);

$$P = JV = (J_{sc} - J_0(e^{\frac{eV}{kT}} - 1))V \quad (3)$$

with J the total current density, V the potential over the absorber material, k Boltzmann's constant, T the temperature of the solar cell and e the elementary charge. The short circuit current density J_{sc} and the reverse saturation current density J_0 are calculated from the absorptivity $\alpha(E)$ of the material using the Equation (4);

$$a(E) = 1 - e^{-2\alpha(E)L} \quad (4)$$

where $a(E)$ the absorptivity for an absorber material, $\alpha(E)$ is the absorption coefficient and L is the thickness of the material with a reflecting back surface. The short circuit current density J_{sc} and the reverse saturation current density J_0 can be calculated by using Equation (5) and (6);

$$J_{sc} = e \int_0^{\infty} a(E) I_{sun} dE \quad (5)$$

$$J_0 = \frac{e\pi}{fr} \int_0^{\infty} a(E) I_{bb} dE \quad (6)$$

where I_{sun} and I_{bb} are AM1.5G solar spectrum and the black body spectrum for room temperature respectively. The fraction of radiative recombination is chosen to be $f_r = 1$, because CZTS material have the characteristic of direct band gap.

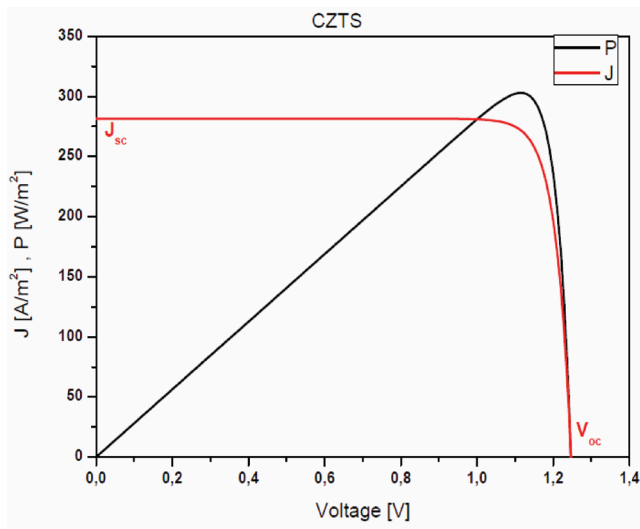


FIGURE 7. J-V characteristic of CZTS

In order to determine the optimized thickness where the material absorbs the totally incident photon, we have calculated the short circuit current density J_{sc} as a function of thickness, as shown in Figure 8. It is clearly shown that the short circuit current density J_{sc} of stannite CZTS become invariant with the increase of thickness of the material after $1 \mu\text{m}$ which indicate that the optimal thickness for CZTS material is $1 \mu\text{m}$ which is in excellent in accordance to the reported value (Olgar et al. 2017). In Figure 7 we presented the J - V characteristic where it is clearly seen that $J_{sc} = 28.14 \text{ mA/cm}^2$ and $V_{oc} = 1.24 \text{ V}$ which mean that the efficiency conversion energy of this material is 30.3% and that's profitable to the photovoltaic application and meet the challenges of low-cost manufacturing of solar cell devices.

THERMOELECTRIC PERFORMANCE

To complete our study, we have also investigated stannite CZTS on thermoelectric properties such as electrical and thermal conductivity, Seebeck coefficient and figure of

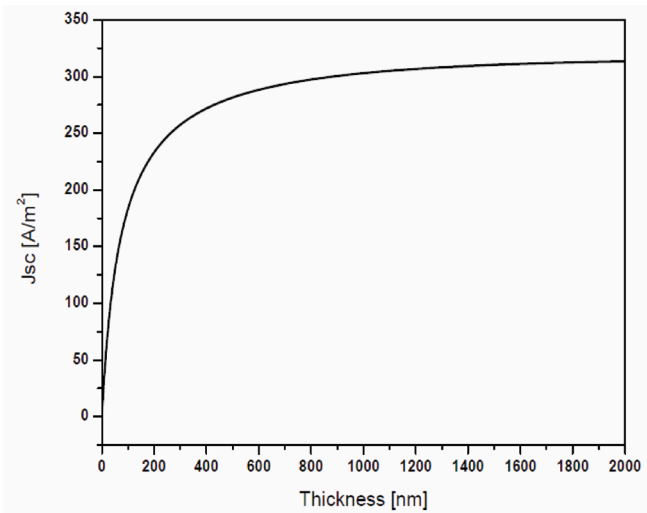


FIGURE 8. The relationship between the thickness and the density short circuit of CZTS

merit, by using Boltztrap code (Madsen et al. 2016) which is based on the semiclassical Boltztrap transport theory and the rigid band approach. However, for the relaxation time which is not obtained by using Boltztrap code, we supposed that the relaxation time is independent with energy. These approaches have been demonstrated to be a reasonably good approximation of several bulk thermoelectric materials (Hammi et al. 2017). In generally, the heat conduction in materials is due by phonon (lattice vibration) and electrons. At low temperature the phonon lattice thermal conductivity is the most dominant, and for higher temperature the electronic thermal conductivity becomes predominant. Therefore, the Boltztrap code calculate only the electronic thermal conductivity.

The thermal conductivity for stannite CZTS is shown in Figure 9, which increases as the temperature increasing and that's because the increasing of temperature lead to increase the probability interaction between electron-electron, and that's is the origin of the increasing of thermal conductivity versus temperature. Also, we show the variation of the charges carriers as function of the temperature. As first remark, we observed that the concentration of charges carriers increase with the increasing of the temperature which provide the characteristic of semiconductor behavior, and the carriers concentration in the room temperature was found to be $8.89 \times 10^{19} \text{ cm}^{-3}$ which is close to the experimental measurement $2.6 \times 10^{19} \text{ cm}^{-3}$ found by Fernandes et al. (2011), the difference between our calculation and the experimental measurement is that in the experimental there's the presence of defect which we did not considered in our study. To determine the nature of these carriers charges we have calculated the Seebeck coefficient. We remark that the Seebeck coefficient is positive which indicates that the charges carriers are holes, which mean that the nature of conduction in stannite CZTS is p -type conduction. A good thermoelectric material is the one which has a higher value of Seebeck coefficient and figure of merit. By definition the Seebeck coefficient indicates the capability of a material to converse a gradient temperature to

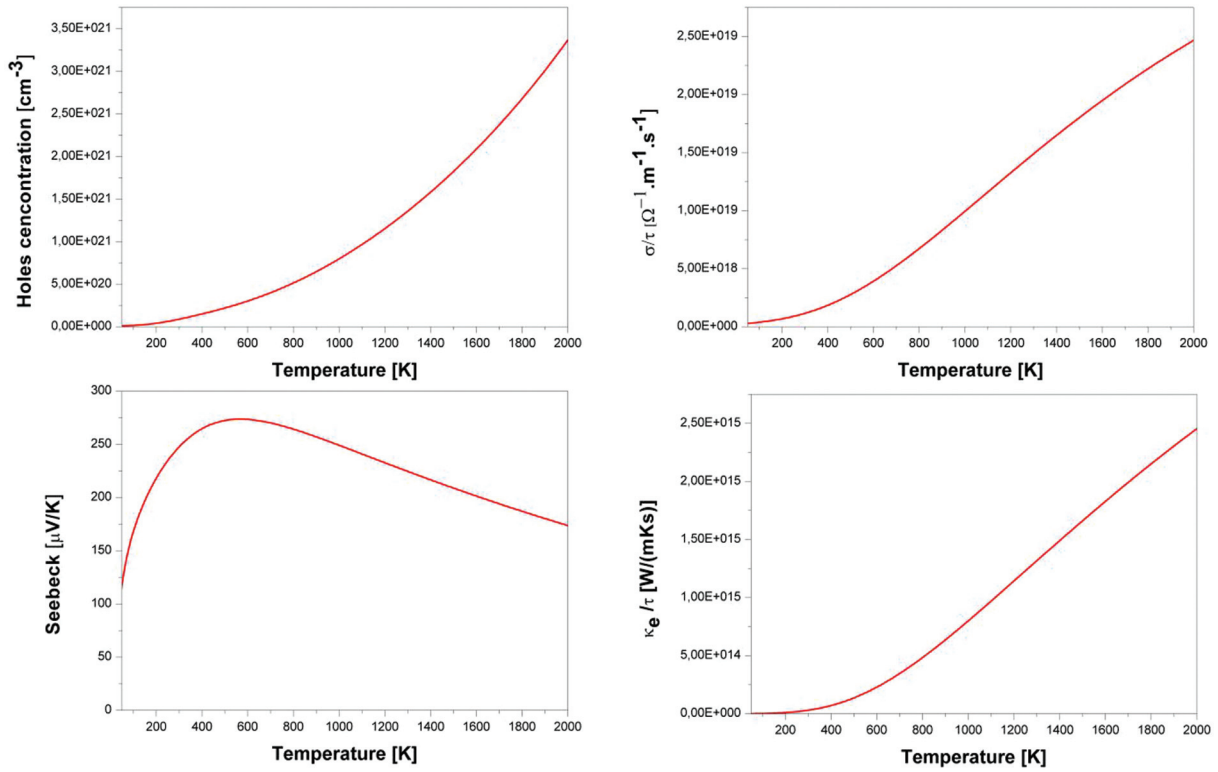


FIGURE 9. Thermoelectric properties of simulated CZTS

voltage. In the room temperature we have found a value of $247 \mu\text{v}/k$, and the Seebeck coefficient increases as increasing the temperature until to achieve a maximum value ($274 \mu\text{v}/k$) at 564 K before started to decrease. Besides, we have plotted the variation of the electrical conductivity, which characterize the flux of free charge carriers. It is worth to mention that, we have found the electrical conductivity increases with the temperature and achieved a value of $1.16 \times 10^{15} \text{ S.cm.}\tau^{-1}$ at room temperature. The electrical conductivity and Seebeck coefficient are associated with each other by the charge carrier concentration. The higher concentration of charge carriers leads to higher electrical conductivity but it reduces the Seebeck coefficient. The same behavior was found in the theoretically work of Haq et al. (2017).

This contrary scenario between these parameters suggest the existence of a particular region where this material has a maximum efficiency of converting heat to electrical, for this reason we have calculated figure of merit see Figure 10, which is calculated by using the Equation (7);

$$ZT = \frac{\sigma S^2 T}{K} \quad (7)$$

where σ , is conductivity electrical, S is Seebeck coefficient, T Temperature, k is thermal conductivity. At the room temperature we have found a value of 0.724, which is close to the value found in $\text{Cu}_2\text{CdSnS}_4$ (0.70) and $\text{Cu}_2\text{CdSnTe}_4$ (0.744) (Hussain et al. 2017). As we expect the figure of merit increase to a certain value of temperature which is 846 K, after the value start dramatically decrease. This could well mean that, this material has better efficiency at thermal

energy under 820 K. Finally, we have calculated the efficiency of converting heat to electricity by using the Equation (8) (Tritt 2011):

$$\eta = \frac{T_h - T_c \sqrt{1 + ZT} - 1}{\sqrt{1 + ZT} + \frac{T_c}{T_h}} \quad (8)$$

where T_c and T_h are the temperatures on the hot and cold sides. By given this equation hot and cold side temperatures of 800 K and 100 K respectively, we found the efficiency conversion thermal is 12.136%.

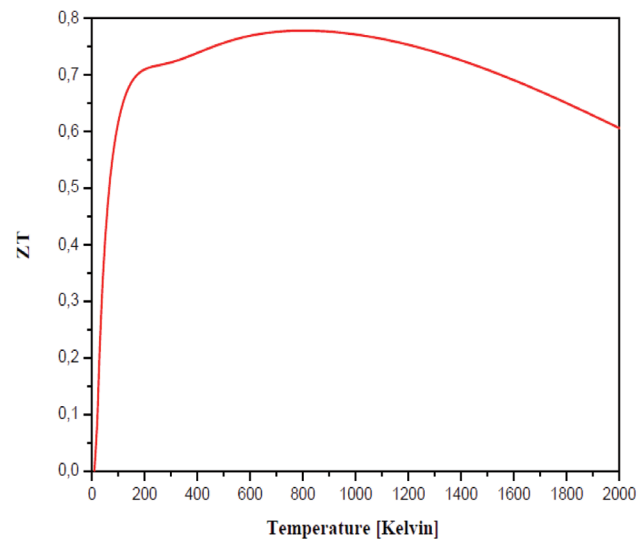


FIGURE 10. Figure of merit of CZTS

CONCLUSION

In summary, we have successfully studied the stannite phase of CZTS. We focus on the crystal structural, electronic structure, optical and thermoelectric properties. This study has been done using DFT+GGA functional implemented in quantum-espresso package. All obtained results are in excellent accord with experimental measurement, such the optical band gap (1.46 eV) and the coefficient absorption (10^5 cm^{-1}) in the visible range, which make this material an excellent candidate to the photovoltaic application. Also, we have calculated the charge carrier concentration of holes ($8.89 \times 10^{19} \text{ cm}^{-3}$), this value for CZTS semiconductor considered close to ideal value proposed by Mott criterion (David & Mott, 1970). Also, we have found figure of merit achieve to a maximum of 0.724 which also considered as good value of *p*-type semiconductor. From this investigation, we suggest that this material can be used as a multi-functional material in different application such as photovoltaic application and thermoelectric.

ACKNOWLEDGEMENT

This work has been supported by the URAC: 08 project PPR: (MESRSFC-CNRST) and also partially supported by Universiti Kebangsaan Malaysia (UKM) Young Researcher Incentive Grant (UKM-GGPM-2016-053). H. Ahmoum would also like to thank UKM for the attachment opportunity in UKM.

REFERENCES

- Anisimov, V.I., Aryasetiawan, F. & Lichtenstein, A.I. 1997. First-principles calculations of the electronic structure and spectra of strongly correlated systems: the LDA+U method. *Journal of Physics: Condensed Matter* 9: 767-808.
- David, A. & Mott, N.F. 1970. Conduction in non-crystalline systems V. Conductivity, optical absorption and photoconductivity in amorphous semiconductors. *Philosophical Magazine* 22(179): 903-922.
- Fernandes, P.A., Salomé, P.M.P. & Cunha, A.F. 2011. Study of polycrystalline $\text{Cu}_2\text{ZnSnS}_4$ films by Raman scattering. *Journal of Alloys and Compounds* 509(28): 7600-7606.
- Giannozzi, P., Baroni, S., Bonini, N., Calandra, M., Car, R., Cavazzoni, C., Ceresoli, D., Chiarotti, G.L., Cococcioni, M., Dabo, I., Dal Corso, A., de Gironcoli, S., Fabris, S., Fratesi, G., Gebauer, R., Gerstmann, U., Gougoussis, C., Kokalj, A., Lazzeri, M., Martin-Samos, L., Marzari, N., Mauri, F., Mazzarello, R., Paolini, S., Pasquarello, A., Paulatto, L., Sbraccia, C., Scandolo, S., Sclauzero, G., Seitsonen, A.P., Smogunov, A., Umari, P. & Wentzcovitch, R.M. 2009. Quantum Espresso: A modular and open-source software project for quantum simulations of materials. *Journal of Physics: Condensed Matter* 21: 395502.
- Gusain, M., Rawat, P. & Nagarajan, R. 2014. Solvent mediated rapid synthesis of orthorhombic $\text{Cu}_2\text{ZnSnS}_4$ (CZTS). *Materials Letters* 133: 220-223.
- Hammi, M., El Rhazouani, O., Arejidal, M. & Slassi, A. 2017. Ab initio study of semi-classic transport coefficient of SnO_2 thermoelectric material. *Chinese Journal of Physics* 55(1): 187-194.
- Haq, B.U., Ahmed, R., Rhee, J., Shaari, A., Alfaifi, S. & Ahmed, M. 2017. Composition-induced influence on the electronic band structure, optical and thermoelectric coefficients of the highly mismatched GaNSb alloy over the entire range: A DFT analysis. *Journal of Alloys and Compounds* 693: 1020-1027.
- Hou, X., Li, Y., Yan, J.J. & Wang, C.W. 2014. Highly efficient photocatalysis of *p*-type $\text{Cu}_2\text{ZnSnS}_4$ under visible-light illumination. *Materials Research Bulletin* 60: 328-633.
- Hussain, S., Murtaza, G., Khan, S.H., Khan, A., Ali, M.A., Faizan, M., Mahmood, A. & Khenata, R. 2016. First principle study of structural, optoelectronic and thermoelectric properties of $\text{Cu}_2\text{CdSnX}_4$ (X = S, Se, Te) chalcogenides. *Materials Research Bulletin* 79: 73-83.
- Jackson, P., Hariskos, D., Wuerz, R., Wischmann, W. & Powalla, M. 2014. Compositional investigation of potassium doped $\text{Cu}(\text{In}, \text{Ga})\text{Se}_2$ solar cells with efficiencies up to 20.8%. *Physica Status Solidi – Rapid Research Letters* 8(3): 219-222.
- Kumar, S., Ansari, M.Z. & Khare, N. 2018. Influence of compactness and formation of metallic secondary phase on the thermoelectric properties of $\text{Cu}_2\text{ZnSnS}_4$ thin films. *Thin Solid Films* 645: 300-304.
- Liu, M.L., Huang, F.Q., Chen, L.D. & Chen, I.W. 2009. A wide band gap *p*-type thermoelectric material based on quaternary chalcogenides of $\text{Cu}_2\text{ZnSnQ}_4$ (Q = S, Se). *Applied Physics Letters* 94(20): 202103.
- Madsen, K.H.G. & Singh, D.J. 2016. BoltzTrap. A Code for calculating band-structure dependent quantities. *Computer Physics Communications* 175(1): 67-71.
- Mahajan, S., Stathatos, E., Huse, N., Birajdar, R., Kalarakis, A. & Sharma, R. 2018. Low cost nanostructure kesterite CZTS thin films for solar cells application. *Materials Letters* 210: 92-96.
- Mohamed, R., Yusop, A.M., Mohamed, A. & Nordin, N.I. 2016. Behavioral analysis of thermoelectric module under different configurations and temperature gradient. *Jurnal Kejuruteraan* 28: 19-27.
- Monkhorst, H.J. & Pack, J.D. 1976. Special points for Brillouin-zone integrations. *Physical Review B* 13: 5188.
- Moukachi, O., Salmani, E., Mahhouthi, Z., Hamedoun, M., Ez-Zahraouy, H., Benaissa, M. & Benyoussef, A. 2014. Accurate band gaps for earth-abundant photovoltaic absorber from density functional theory. In: *International Renewable and Sustainable Energy Conference (IRSEC)*, IEEE. 1498548.
- Olgar, M.A., Klaer, J., Mainz, R., Ozyuzer, L. & Unold, T. 2017. $\text{Cu}_2\text{ZnSnS}_4$ -based thin films and solar cells by

- rapid thermal annealing processing. *Thin Solid Films* 628: 1-6.
- Park, K.T., Shin, S.M., Tazebay, A.S., Um, H.D., Jung, J.Y., Jee, S.W., Oh, M.W., Park, S.D., Yoo, B., Yu, C. & Lee, J.H. 2013. Lossless hybridization between photovoltaic and thermoelectric devices. *Scientific Reports* 3: 2123.
- Perdew, J.P., Burke, K. & Ernzerhof, M. 1996. Generalized gradient approximation made simple. *Physical Review Letters* 77: 3865.
- Quennet, M., Ritscher, A., Lerch, M. & Paulus, B. 2017. The order-disorder transition in $\text{Cu}_2\text{ZnSnS}_4$: A theoretical and experimental study. *Journal of Solid State Chemistry* 250: 140-144.
- Reshak, A.H., Nouneh, K., Kityk, I.V., Bila, J., Auluck, S., Kamarudin, H. & Sekkat, Z. 2014. Structural, electronic and optical Properties in earth-abundant photovoltaic absorber of $\text{Cu}_2\text{ZnSnS}_4$ and $\text{Cu}_2\text{ZnSnS}_4$ from DFT calculation. *International Journal of Electrochemical Science* 9: 955-974.
- Ricardo, C.L.A, Su'ait, M.S., Müller, M. & Scardi, P. 2013. Production of $\text{Cu}_2(\text{Zn, Fe})\text{SnS}_4$ powders for thin solar cell by high energy ball milling. *Journal of Power Sources* 230: 70-75.
- Sakib, N. & Ahad, M.A.R. 2018. An optimized structure for enhancing optical absorption of solar energy in elliptical GaAs nanowire array solar cell. *Jurnal Kejuruteraan* 30(1): 1-6.
- Tritt, T.M. 2011. Thermoelectric phenomena, materials and applications. *Annual Review Materials Research* 41: 433-448.
- Wang, H., Bahk, J.H., Kang, C., Hwang, J., Kim, K., Shakouri, A. & Kim, W. 2013. Large enhancement in the thermoelectric properties of $\text{Pb}_{0.98}\text{Na}_{0.02}\text{Te}$ by optimizing the synthesis condition. *Journal of Materials Chemistry A* 1: 11269-11278.
- Zhao, Y., Li, D. & Liu, Z. 2017. Structural and elastic DFT study of four structures for $\text{Cu}_2\text{ZnSnS}_4$ under high pressure. *Journal of Alloys and Compounds* 696: 86-95.
- *Hassan Ahmoum, Mourad Boughrara,
Mohamed Kerouad
Laboratoire de Physique des Matériaux et Modélisation des Systèmes (LP2MS), Unité Associée au CNRST-URAC: 08, Faculty of Sciences, Moulay Ismail University, B.P. 11201, Zitoune, Morocco
- Puvaneswaran Chelvanathan, Kamaruzzaman Sopian,
*Mohd Sukor Su'ait
Solar Energy Research Institute (SERI),
Universiti Kebangsaan Malaysia,
43600 Bangi, Selangor, Malaysia.
- *Lee Tian Khoon
Fuel Cell Institute, Universiti Kebangsaan Malaysia,
43600, Bangi, Selangor, Malaysia.
- Baohai Jia, Guojian Li
Key Laboratory of Electromagnetic Processing of Materials (Ministry of Education), Northeastern University, Shenyang 110004, China
- *Corresponding author; email:
h.ahmoum@gmail.com
mohdsukor@ukm.edu.my
- Received date: 9th June 2018
Accepted date: 22nd July 2018
Online first date: 1st October 2018
Published date: 30th November 2018